Fourth-Order Partial Differential Equations for Noise Removal

Yu-Li You, *Member, IEEE,* and M. Kaveh, *Fellow, IEEE*

***Abstract*—A class of fourth-order partial differential equations (PDEs) are proposed to optimize the trade-off between noise removal and edge preservation. The time evolution of these PDEs seeks to minimize a cost functional which is an increasing function of the absolute value of the Laplacian of the image intensity function. Since the Laplacian of an image at a pixel is zero if the image is planar in its neighborhood, these PDEs attempt to remove noise and preserve edges by approximating an observed image with a piecewise planar image. Piecewise planar images look more natural than step images which anisotropic diffusion (second order PDEs) uses to approximate an observed image. So the proposed PDEs are able to avoid the blocky effects widely seen in images processed by anisotropic diffusion, while achieving the degree of noise removal and edge preservation comparable to anisotropic diffusion. Although both approaches seem to be comparable in removing speckles in the observed images, speckles are more visible in images processed by the proposed PDEs, because piecewise planar images are less likely to mask speckles than step images and anisotropic diffusion tends to generate multiple false edges. Speckles can be easily removed by simple algorithms such as the one presented in this paper.**

***Index Terms*—Anisotropic diffusion, fourth order PDEs, image smoothing, piecewise planar images.**

I. Introduction

SECOND order partial differential equations (PDE) have been studied as a useful tool for image enhancement (noise removal) and scale-space analysis of images. They include anisotropic diffusion equations as formulated in [1]–[3] and derived from total variation minimization (see [4], [5] for example) as well as curve evolution equations that are based on geometric heat flow of the level sets of the image (see [6]–[10], for example).

Although these techniques have been demonstrated to be able to achieve a good trade-off between noise removal and edge preservation, they tend to cause the processed image to look "blocky" as can be seen from the images in [1], [4] and especially as reported in [11]. This effect is visually unpleasant and is likely to cause a computer vision system to falsely recognize as edges the boundaries of different blocks that actually belong to the same smooth area in the original image.

Manuscript received May 13, 1999; revised April 27, 2000. This work was supported in part by the National Science Foundation under Grant CDA-9414015. The associate editor coordinating the review of this manuscript and approving it for publication was Prof. Scott T. Acton.

Y.-L. You is with Digital Theater Systems, Inc., Agoura Hills, CA 91301 USA.

M. Kaveh is with the Department of Electrical and Computer Engineering, University of Minnesota, Minneapolis, MN 55455 USA (e-mail: kaveh@ece.umn.edu).

Publisher Item Identifier S 1057-7149(00)07596-5.

This blocky effect is, to a large extent, inherent in the nature of all these equations, which are second order. Since second order derivatives are zero only if the image intensity function is planar, these types of PDEs will evolve toward and settle down to a planar image if the image support is infinite. For images of limited support, however, symmetric boundary condition is usually employed in order to avoid distortion at the boundaries. By symmetric boundary condition, we mean that the image intensity function has equal values at both sides of the boundary. Since the image gradient is obviously zero at these boundaries, an image will evolve toward a level (horizontally planar) image to satisfy this boundary condition of zero gradient. In order to preserve edges while removing noise, this kind of PDEs are usually designed to evolve faster in smooth areas than around edges. Therefore, after certain time of evolution, the image will look like one consisting of level areas of various intensities. The boundaries of these level areas may coincide with edges, but may appear in the middle of large smooth and slant areas, as well.

A rather detailed analysis of blocky effects associated with anisotropic diffusion was carried out in [12]. Let u denote the image intensity function, t the time, and $c(\cdot)$ the diffusion coefficient, the anisotropic diffusion as formulated in [1] may be presented as

$$\frac{\partial u}{\partial t} = \text{div}\,(c(|\nabla u|)\nabla u). \tag{1}$$

This equation was associated with the following energy functional

$$E(u) = \int_{\Omega} f(|\nabla u|)\, d\Omega \tag{2}$$

where Ω is the image support, and $f(\cdot) \geq 0$ is an increasing function associated with the diffusion coefficient as

$$c(s) = \frac{f'(s)}{s}. \tag{3}$$

Anisotropic diffusion is then shown to be an energy-dissipating process that seeks the minimum of the energy functional. From (2), it is obvious that level images are global minima of the energy functional. Detailed analysis indicates that, when there is no backward diffusion, a level image is the only minimum of the energy functional, so anisotropic diffusion will evolve toward the formation of a level image function. Since anisotropic diffusion is designed such that smooth areas are diffused faster than less smooth ones, blocky effects will appear in the early stage of diffusion, even though all the blocks will finally merge to form

a level image. When there is backward diffusion, however, any step image (piecewise level image) [1] is a global minimum of the energy functional, so blocks will appear in the early stage of the diffusion and will remain as such.

This paper proposes the use of fourth-order PDEs as a technique to avoid blocky effects while achieving good tradeoff between noise removal and edge preservation. In particular, Section II derives a family of fourth-order PDEs from a functional which is an increasing function of the Laplacian of the image intensity function [13]. Since the Laplacian of an image at a pixel is zero if the image is planar in its neighborhood, these PDEs attempt to remove noise and preserve edges by approximating an observed image with a piecewise planar image. A similar idea was pursued in [14] for contrast enhancement, resulting in a set of fourth-order PDEs which is more complex than that presented in [13] and here. Section III presents a numerical implementation of the proposed fourth-order PDE. Section IV develops an algorithm to alleviate speckle effects that is likely to appear in the processed image. Numerical examples are presented in Section V and the paper is concluded in Section VI.

II. Fourth Order PDEs

Let us first consider the following functional defined in the space of continuous images over a support of Ω

$$E(u) = \int_{\Omega} f(|\nabla^2 u|)\, dx\, dy \tag{4}$$

where ∇^2 denotes Laplacian operator. We require that the function $f(\cdot) \geq 0$ and is an increasing function

$$f'(\cdot) > 0 \tag{5}$$

so that the functional is an increasing function with respect to the smoothness of the image as measured by $|\nabla^2 u|$. Therefore, the minimization of the functional is equivalent to smoothing the image.

This functional minimization is a special form of the general variational problem treated in [15]

$$E(u) = \int_{\Omega} F(x, y, u, D_1 u, D_2 u, \cdots, D_i u, \cdots)\, dx\, dy \tag{6}$$

where

$$D_i u = \left[\frac{\partial^i u}{\partial x^i}, \frac{\partial^i u^i}{\partial y^i}\right]^T. \tag{7}$$

The equivalent Euler equation is

$$\sum D_i^T \left(\frac{\partial F}{\partial D_i u}\right) = 0 \tag{8}$$

where $D_i^T = -D_i$ for derivatives of odd order and $D_i^T = +D_i$ for even derivatives. For our special case, we have

$$F(u_{xx}, u_{yy}) = f(|\nabla^2 u|) = f(|u_{xx} + u_{yy}|). \tag{9}$$

[1] A step image is the sum of a finite number of dislocated two-dimensional step functions.

We can easily derive that

$$\frac{\partial F}{\partial u_{xx}} = \frac{\partial F}{\partial u_{yy}} = f'(|\nabla^2 u|)\ \text{sign}\ (\nabla^2 u) \tag{10}$$

where

$$\text{sign}\ (s) = \begin{cases} -1, & s < 0 \\ 0, & s = 0 \\ 1, & s > 0 \end{cases} \tag{11}$$

and

$$f'(s) = \frac{\partial f}{\partial s}. \tag{12}$$

Therefore, the Euler equation is

$$\nabla^2 [f'(|\nabla^2 u|)\ \text{sign}\ (\nabla^2 u)] = 0 \tag{13}$$

which is

$$\nabla^2 \left[f'(|\nabla^2 u|)\frac{\nabla^2 u}{|\nabla^2 u|}\right] = 0 \tag{14}$$

if we define

$$\left.\frac{\nabla^2 u}{|\nabla^2 u|}\right|_{\nabla^2 u = 0} = 0. \tag{15}$$

Using (3), we may represent (14) as

$$\nabla^2 \left[c(|\nabla^2 u|)\nabla^2 u\right] = 0. \tag{16}$$

The Euler equation may be solved through the following gradient descent procedure:

$$\frac{\partial u}{\partial t} = -\nabla^2 \left[f'(|\nabla^2 u|)\frac{\nabla^2 u}{|\nabla^2 u|}\right] = -\nabla^2 [c(|\nabla^2 u)\nabla^2 u] \tag{17}$$

with the observed image as the initial condition. The solution is arrived when $t \to \infty$, but the time evolution may be stopped earlier to achieve an optimal tradeoff between noise removal and edge preservation. A related fourth-order diffusion equation and its properties are discussed in [18].

Let us refer to an image whose intensity function satisfies the equation of a plane as a planar image. The Laplacian of such an image is zero, so it satisfies the Euler equation (16). Therefore, a planar image is a stationary point of the Euler equation (16).

Furthermore, we can show that a planar image is a global minimum of the cost functional $E(u)$. Due to the nonnegativity of $f(|\nabla^2 u|)$, the functional $E(u)$ is bounded below:

$$E(u) \geq 0. \tag{18}$$

Since $f(|\nabla^2 u|)$ is an increasing function of $|\nabla^2 u|$, its global minimum is at $|\nabla^2 u| = 0$. Consequently, the global minimum of $E(u)$ occurs when

$$|\nabla^2 u| \equiv 0 \quad \text{for all } (x, y) \in \Omega. \tag{19}$$

A planar image obviously satisfies (19), hence is a global minimum of $E(u)$.

Planar images are the only global minimum of $E(u)$ if $f(\cdot)$ is convex, or equivalently if

$$f''(s) \geq 0, \quad \text{for all } s \geq 0 \tag{20}$$

because the cost functional $E(u)$ is convex under this condition (see Appendix A). Therefore, the evolution of (17) is a process in which the image is smoothed more and more until it becomes a planar image.

On the other hand, if condition (20) is not satisfied, i.e., $f''(s) < 0$ for some or all $s \geq 0$, the cost functional $E(u)$ may not be convex. So there may exist other local and/or global minima. In the following, we show that piecewise planar images are such minima.

Let $\Omega_i, i = 1, 2, \cdots, n$, be a partition of Ω. We define a piecewise planar image as

$$s(x,y) = \sum_{i=1}^{n} s_i(x,y) \tag{21}$$

where

$$s_i(x,y) = \begin{cases} \text{planar image}, & (x,y) \in \Omega_i \\ 0, & \text{otherwise.} \end{cases} \tag{22}$$

We require that the planar images in (22) be such that the combined image $s(x,y)$ is continuous. Note that any two adjacent $s_i(x,y)$ and $s_j(x,y)$ must be on different planes; otherwise, we can combine them as one. Let us denote $\partial\Omega_i$ as the boundary of partition Ω_i, then $\Omega_i - \partial\Omega_i$ is the interior of Ω_i. It is obvious that

$$\nabla s_i(x,y) = \text{constant}, \qquad (x,y) \in (\Omega_i - \partial\Omega_i) \tag{23}$$

so we have

$$\nabla^2 s_i(x,y) = 0, \qquad (x,y) \in (\Omega_i - \partial\Omega_i) \tag{24}$$

for $i = 1, 2, \cdots, n$. Therefore,

$$\nabla^2 s(x,y) = 0, \qquad (x,y) \in (\Omega - \partial\Omega) \tag{25}$$

where $\partial\Omega = \cup_{i=1}^{n} \partial\Omega_i$. Since it is required that any two adjacent s_i and s_j be on different planes, we have

$$\nabla s_i \neq \nabla s_j \tag{26}$$

for any two adjacent partitions Ω_i and Ω_j. This indicates that the gradient is not continuous at the boundary $\partial\Omega$. So, we have

$$\nabla^2 s(x,y) = \infty, \quad \text{for all } (x,y) \in \partial\Omega. \tag{27}$$

If we require that

$$f'(\infty) = 0 \tag{28}$$

we then have

$$f'(|\nabla^2 u|)\frac{\nabla^2 u}{|\nabla^2 u|} = 0 \quad \text{for all } (x,y) \in \Omega. \tag{29}$$

Therefore, a piecewise planar image satisfies the Euler equation.

Due to condition (5), (28) indicates that it is impossible for $f(\cdot)$ to satisfy (20). Therefore, (28) implies that

$$f''(s) < 0, \quad \text{for some } s \tag{30}$$

or equivalently, $f(\cdot)$ is not convex.

As discussed in [12], (28) or (30) is the condition for anisotropic diffusion to evolve an observed image toward a step image (piecewise level image) and is, therefore, the major reason for anisotropic diffusion to suffer from blocky effects. The proposed fourth-order PDE, however, evolves an observed image toward a piecewise planar image which, we believe, is a better approximation to natural images. Therefore, the processed image will look less blocky and more natural.

III. Difference Equation

The differential equation (17) may be solved numerically using an iterative approach. Assuming a time step size of Δt and a space grid size of h, we quantize the time and space coordinates as follows:

$$t = n\Delta t, \qquad n = 0, 1, 2, \cdots \tag{31}$$

$$x = ih, \qquad i = 0, 1, 2, \cdots I \tag{32}$$

$$y = jh, \qquad j = 0, 1, 2, \cdots J \tag{33}$$

where $Ih \times Jh$ is the size of image support. We then employ a three-stage approach to calculate the right hand side of (17). At the first stage, we calculate the Laplacian of the image intensity function as

$$\nabla^2 u_{i,j}^n = \frac{u_{i+1,j}^n + u_{i-1,j}^n + u_{i,j+1}^n + u_{i,j-1}^n - 4\,u_{i,j}^n}{h^2} \tag{34}$$

with symmetric boundary conditions

$$u_{-1,j}^n = u_{0,j}^n, \quad u_{I+1,j}^n = u_{I,j}^n, \qquad j = 0, 1, 2, \cdots, J \tag{35}$$

and

$$u_{i,-1}^n = u_{i,0}^n, \quad u_{i,J+1}^n = u_{i,J}^n, \qquad i = 0, 1, 2, \cdots, I. \tag{36}$$

At the second stage, we calculate the value of the following function:

$$g(\nabla^2 u) = f'(|\nabla^2 u|)\frac{\nabla^2 u}{|\nabla^2 u|} = c(|\nabla^2 u|)\nabla^2 u \tag{37}$$

as

$$g_{i,j}^n = g(\nabla^2 u_{i,j}^n). \tag{38}$$

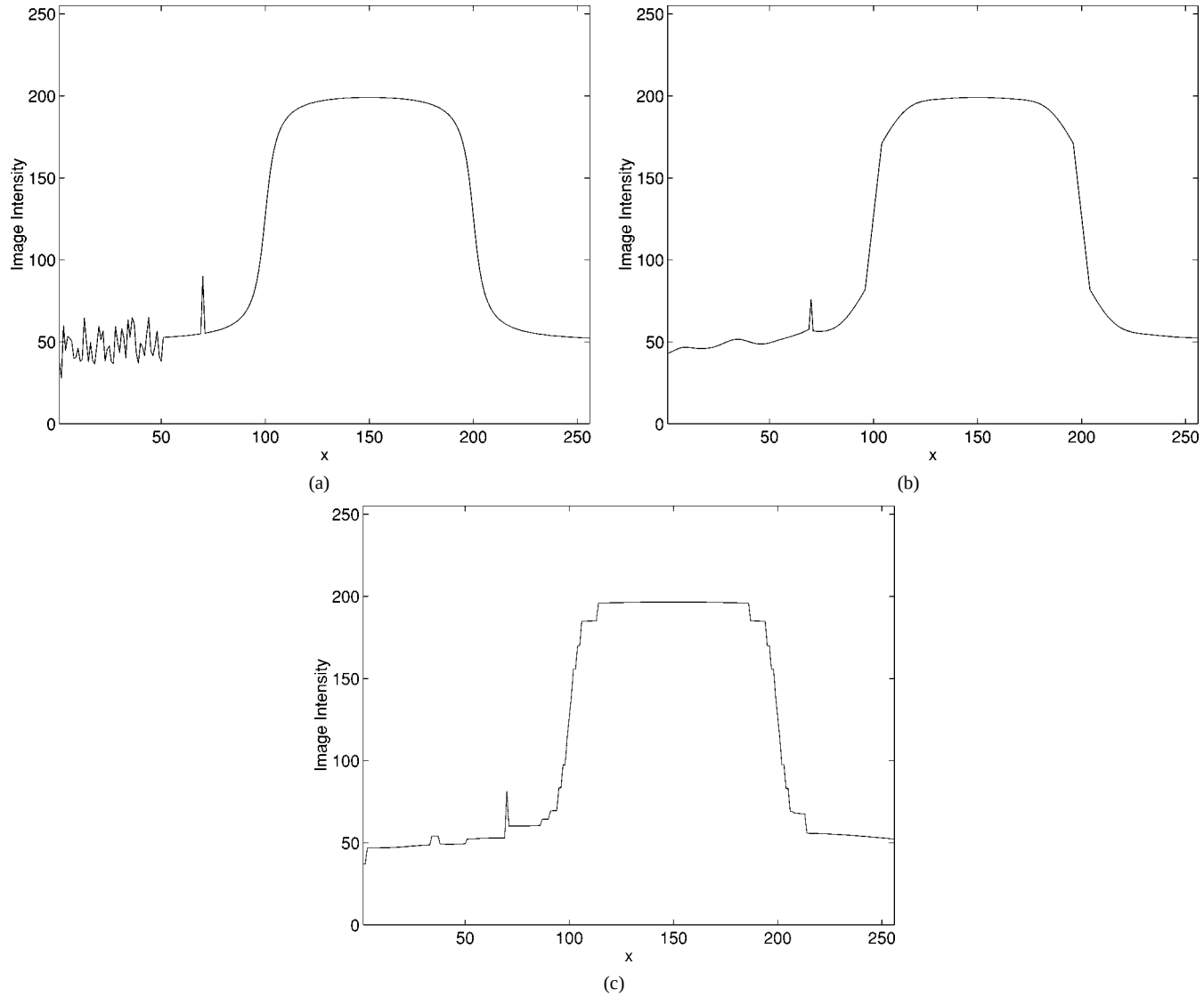

Fig. 1. (a) Original image, (b) image processed by the proposed fourth-order PDE at $t = 500$, and (c) image processed by anisotropic diffusion at $t = 500$.

At the third stage, we calculate the Laplacian of $g(\cdot)$ as

$$\nabla^2 g^n_{i,j} = \frac{g^n_{i+1,j} + g^n_{i-1,j} + g^n_{i,j+1} + g^n_{i,j-1} - 4g^n_{i,j}}{h^2} \quad (39)$$

with symmetric boundary conditions

$$g^n_{-1,j} = g^n_{0,j}, \quad g^n_{I+1,j} = g^n_{I,j}, \qquad j = 0, 1, 2, \cdots, J \quad (40)$$

and

$$g^n_{i,-1} = g^n_{i,0}, \quad g^n_{i,J+1} = g^n_{i,J}, \qquad i = 0, 1, 2, \cdots, I. \quad (41)$$

Finally, the numerical approximation to the differential equation (17) is given as

$$u^{n+1}_{i,j} = u^n_{i,j} - \Delta t \nabla^2 g^n_{i,j}. \quad (42)$$

There is an issue of choosing the optimal step size Δt which would ensure speedy convergence. Due to the severe nonlinearity of the equation, however, such an optimal step size is difficult to obtain theoretically and very expensive computationally. Instead, we took an experimental approach and found that a good step size is 0.25.

IV. Despeckle Algorithm

The proposed PDEs tend to leave the processed images with isolated black and white speckles which may be characterized as pixels whose intensity values are either much larger or smaller than those of their neighboring pixels. This phenomenon may be explained as follows. Since the Laplacian of the image intensity function is very large around speckle pixels and the function $f(\cdot)$ is designed such that it decreases rapidly in order to preserve edges, the function $g(\cdot)$ defined in (37) will have small values around speckle pixels. Then the right-hand side of (17) will be very small. Consequently, the speckles are likely to be left intact, just as the edges are.

This type of isolated speckles can be removed with simple algorithms such as median filters [17]. In order to exploit the special property that such speckles have significantly larger or smaller intensity values than their neighboring pixels, we present the following algorithm. Denote the mean and variance of the neighboring pixels around a pixel (i, j) as

$$m = \frac{u_{i,j-1} + u_{i,j+1} + u_{i-1,j} + u_{i+1,j}}{4} \quad (43)$$

(a) (b)

Fig. 2. (a) Original image and (b) degraded by 10 dB Gaussian noise.

(a) (b)

Fig. 3. Images processed by fourth-order PDE at (a) $t = 500$ and (b) $t = 1000$.

and

$$\sigma^2 = \frac{u_{i,j-1}^2 + u_{i,j+1}^2 + u_{i-1,j}^2 + u_{i+1,j}^2}{4} - m^2. \tag{44}$$

Then, this pixel is a speckle if σ is small and $|u_{i,j} - m| \gg \sigma$. Therefore, the proposed despeckle algorithm is

$$u_{i,j} = \begin{cases} m, & \text{if } |u_{i,j} - m|^2 > k\sigma^2; \\ u_{i,j}, & \text{otherwise;} \end{cases} \tag{45}$$

where k is a constant that may be adjusted for a specific application.

V. Numerical Examples

We now demonstrate the performance of the proposed fourth-order PDE. We use the difference scheme discussed in Section III to process degraded images and compare the results with those processed using anisotropic diffusion with a difference

(a) (b)

Fig. 4. Removal of the speckle artifacts in the images processed by fourth-order PDE (Fig. 3).

(a) (b)

Fig. 5. Images processed by anisotropic diffusion at (a) $t = 100$ and (b) $t = 200$.

scheme discussed in [4] and [12]. For both PDEs, we use the following function [1]

$$c(s) = \frac{1}{1+(s/k)^2}. \tag{46}$$

We use step size $\Delta t = 0.25$ and grid size $h = 1$.

We first consider a one-dimensional computer-generated image shown at top of Fig. 1. It consists of a section of Gaussian noise, an isolated speckle noise, and two smooth edges. This image is fed into the fourth-order PDE as initial condition and the time evolution of this PDE begins. We set $k = 0.5$ for the $c(\cdot)$ in (46). The processed image at $t = 500$ is shown at middle of Fig. 1. For comparison, we show the image processed by anisotropic diffusion under exactly the same condition at bottom of Fig. 1. The difference between the proposed fourth-order PDE and anisotropic diffusion are obvious: while anisotropic approximates the observed image with a step image, the proposed fourth-order PDE with a piecewise planar image

which looks more natural and does not produce false edges. We note that neither approach handles isolated speckle noise well.

We now consider a two-dimensional image. The image shown at the top of Fig. 2 is degraded to give the image at the bottom of Fig. 2 using Gaussian noise at a SNR = 10 dB, where

$$\text{SNR} = \frac{\text{Variance of image}}{\text{Variance of noise}}. \tag{47}$$

This degraded image is then fed into the fourth-order PDE as initial condition and the time evolution of this PDE begins. Fig. 3 shows two images generated by the fourth-order PDE when $t = 200$ and $t = 1000$. Since these two images suffer from speckle artifacts, they are further processed by the despeckle algorithm ($k = 3$) presented in Section IV to give the images in Fig. 4. For comparison, Fig. 5 shows the images processed by anisotropic diffusion when $t = 100$ and $t = 200$. The blocky effects are obvious in these two images. Although speckle artifacts do not seem to be a major problem in these two images, a closer look indicates that the speckles still exist but are largely masked by the blockiness. Fig. 1 strongly indicates that both the proposed PDE and anisotropic diffusion are comparable in removing speckles, but speckles are more visible in images processed by the proposed PDE because step images have stronger masking capability than piecewise planar ones and anisotropic diffusion tends to generate multiple false edges.

VI. Conclusion

A class of fourth-order PDEs were derived as a process that seeks to minimize a functional proportional to the absolute value of the Laplacian of the image intensity function. It was shown that the time evolution of these PDEs will converge to piecewise planar images which look more natural than the step images that are the stationary points of anisotropic diffusion (second order PDEs). Both the proposed PDE and anisotropic diffusion seem to be comparable in removing speckles in the observed images, but speckles are more visible in images processed by the proposed PDE because piecewise planar images have less masking capability than step images and anisotropic diffusion tends to generate multiple false edges. Speckles can be easily removed by simple algorithms such as the one presented in this paper.

Appendix I
Convexity of the Cost Functional

Let u_1 and u_2 be two images defined on support Ω with $u_1 \neq u_2$, then for each $\lambda \in (0,1)$ we have by Minkowski inequality [16]

$$|\nabla^2[\lambda u_1 + (1-\lambda)u_2]| \leq \lambda|\nabla^2 u_1| + (1-\lambda)|\nabla^2 u_2|. \tag{48}$$

Since $f(\cdot)$ is strictly increasing [please refer to (5)] and (48) gives

$$f(|\nabla^2[\lambda u_1 + (1-\lambda)u_2]|) \leq f(\lambda|\nabla^2 u_1| + (1-\lambda)|\nabla^2 u_2|). \tag{49}$$

The convexity of $f(\cdot)$ gives

$$f(\lambda|\nabla^2 u_1| + (1-\lambda)|\nabla^2 u_2|) \leq \lambda f(|\nabla^2 u_1|) + (1-\lambda) f(|\nabla^2 u_2|). \tag{50}$$

Combining (49) and (50), we have

$$f(|\nabla^2[\lambda u_1 + (1-\lambda)u_2]|) \leq \lambda f(|\nabla^2 u_1|) + (1-\lambda) f(|\nabla^2 u_2|). \tag{51}$$

Integrating (51) gives

$$\int_\Omega |\nabla[\lambda u_1 + (1-\lambda)u_2]| d\Omega \leq \lambda \int_\Omega f(|\nabla u_1|)\, d\Omega + (1-\lambda) \int_\Omega f(|\nabla u_2|)\, d\Omega \tag{52}$$

which is

$$E(\lambda u_1 + (1-\lambda)u_2) \leq \lambda E(u_1) + (1-\lambda)E(u_2). \tag{53}$$

Therefore, the functional $E(u)$ is convex.

References

[1] P. Perona and J. Malik, "Scale-space and edge detection using anisotropic diffusion," *IEEE Trans. Pattern Anal. Machine Intell.*, vol. 12, pp. 629–639, July 1990.

[2] F. Catte, P.-L. Lions, J.-M. Morel, and T. Coll, "Image selective smoothing and edge detection by nonlinear diffusion," *SIAM J. Numer. Anal.*, vol. 29, pp. 182–193, Feb. 1992.

[3] S. Kichenassamy, *Edge Localization via Backward Parabolic and Hyperbolic PDE*. Minneapolis, MN: Univ. Minnesota.

[4] L. I. Rudin, S. Osher, and E. Fatemi, "Nonlinear total variation based noise removal algorithms," *Physica D*, vol. 60, pp. 259–268, 1992.

[5] C. Vogel and M. Oman, "Iterative methods for total variation denoising," *SIAM J. Sci. Statist. Comput.*, vol. 17, pp. 227–238, 1996.

[6] B. Kimia, A. Tannenbaum, and S. Zucker, "On the evolution of curves via a function of curvature I," *J. Math. Anal. Applicat.*, vol. 163, pp. 438–458, 1992.

[7] S. J. Osher and J. A. Sethian, "Fronts propagating with curvature dependent speed: Algorithms based on hamilton-jacobi formulations," *J. Comput. Phys.*, vol. 79, pp. 12–49, 1988.

[8] J. A. Sethian, "Curvature and the evolution of fronts," *Commun. Math. Phys.*, vol. 101, pp. 487–499, 1985.

[9] B. Kimia, A. Tannenbaum, and S. Zucker, "Toward a computational theory of shape: An overview," McGill University, Montreal, PQ, Canada, Tech. Rep. Cim-89-13, 1989.

[10] G. Sapiro and A. Tannenbaum, "Affine invariant scale-space," *Int. J. Comput. Vis.*, vol. 11, no. 1, pp. 25–44, 1993.

[11] R. T. Whitaker and S. M. Pizer, "A multi-scale approach to nonuniform diffusion," *Comput. Vis. Graph. Image Process.: Image Understand.*, vol. 57, pp. 99–110, Jan. 1993.

[12] Y.-L. You, W. Xu, A. Tannenbaum, and M. Kaveh, "Behavioral analysis of anisotropc diffusion in image processing," *IEEE Trans. Image Processing*, vol. 5, pp. 1539–1553, Nov. 1996.

[13] Y.-L. You and M. Kaveh, "Image enhancement using fourth order partial differential equations," in *32nd Asilomar Conf. Signals, Systems, Computers*, vol. 2, 1998, pp. 1677–1681.

[14] J. Tumblin and G. Turk, "LCIS: A boundary hierarchy for detail-preserving contrast reduction," in *SIGGRAPH 1999 Annu. Conf. Computer Graphics*, Los Angeles, Aug. 8–13, 1999, pp. 83–90.

[15] G. Strang, *Introduction to Applied Mathematics*. Cambridge, MA: Wellesley-Cambridge.

[16] A. W. Naylor and G. R. Sell, *Linear Operator Theory in Engineering and Science*. Berlin, Germany: Springer-Verlag, 1982.

[17] R. C. Gonzalez and R. E. Woods, *Digital Image Processing*. Reading, MA: Addison-Wesley, 1992.

[18] A. L. Bertozzi, "The mathematics of moving contact lines in thin liquid films," *Notices AMS*, vol. 45, pp. 689–697, June/July 1998.

Yu-Li You (S'95–M'97) received B.S and M.S. degrees in electronic engineering from Xidian University, Northwestern Telecommunication Engineering Institute, Xi'an, China, in 1985 and 1988, respectively, and the Ph.D degree in electrical engineering from the University of Minnesota, Minneapolis, in 1995.

He was a Senior Software Engineer with Seagate Technology, Inc., from 1995 to 1996 and an Adjunct Assistant Professor with the Department of Electrical Engineering, University of Minnesota, from 1996 to 1998. He has been a Senior Engineer with Digital Theater Systems, Inc., Agoura Hills, CA, since 1996. His research interests include real-time DSP software/hardware development, audio/video compression, image enhancement, image restoration, image analysis, communications, and neural networks.

Dr. You received 1990 Science and Technology Award from Guangdong Provincial Government of China.

M. Kaveh (S'73–M'75–SM'83–F'88) received the B.S. degree in electrical engineering from Purdue University, West Lafayette, IN, in 1969, the M.S. degree from the University of California, Berkeley, in 1970, and the Ph.D. degree from Purdue in 1974.

He is has been with the University of Minnesota, Minneapolis, since 1975. He is currently a Professor and Head of the Department of Electrical and Computer Engineering.

Dr. Kaveh is former member of the Board of Governors and a past Vice President for Publications of the IEEE Signal Processing Society and was the General Chairman of ICASSP'93. He received the 1986 ASSP Senior Best Paper Award (with A. Barabell) and the 1988 ASSP Meritorious Service Award.